Biofabrication

International Society for Biofabrication

PAPER

Mouse *in vitro* spermatogenesis on alginate-based 3D bioprinted scaffolds

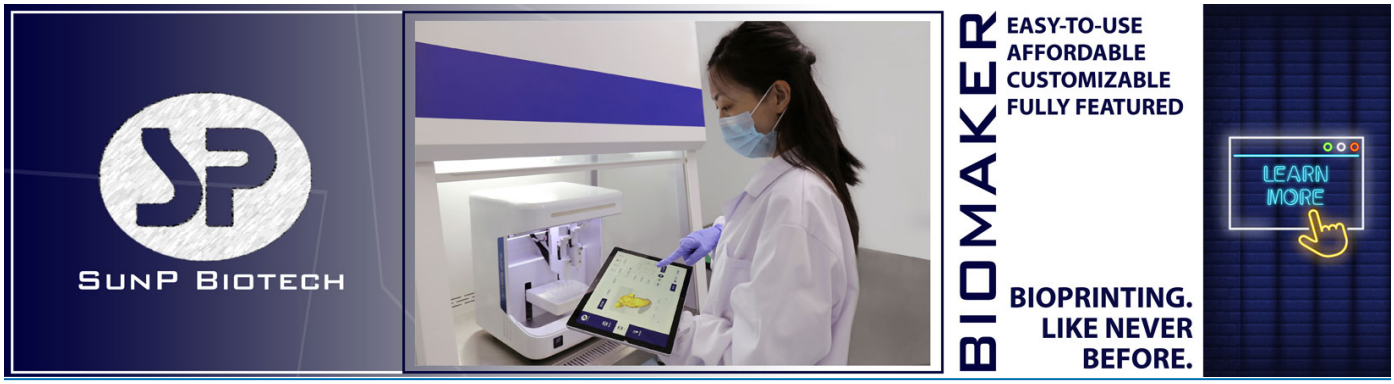

Biofabrication

PAPER

Mouse *in vitro* spermatogenesis on alginate-based 3D bioprinted scaffolds

RECEIVED
16 October 2018

REVISED
21 March 2019

ACCEPTED FOR PUBLICATION
28 March 2019

PUBLISHED
26 April 2019

Yoni Baert[1,2], **Katerina Dvorakova-Hortova**[3,4], **Hasmik Margaryan**[3] **and Ellen Goossens**[1]

[1] Biology of the Testis, Research Laboratory for Reproduction, Genetics and Regenerative Medicine, Vrije Universiteit Brussel (VUB), Laarbeeklaan 103, B-1090 Brussels, Belgium
[2] Polymer Chemistry & Biomaterials Research Group, Department of Organic Chemistry, Ghent University, Krijgslaan 281 S4 Bis, B-9000 Ghent, Belgium
[3] Group of Reproductive Biology, Institute of Biotechnology CAS, v.v.i., BIOCEV, Prumyslova 595, 252 50, Vestec, Czech Republic
[4] Department of Zoology, Faculty of Science, Charles University, Vinicna 7, Prague 2, 128 44, Czech Republic

E-mail: yoni.baert@vub.be

Keywords: spermatogonial stem cells, testis, *in vitro* spermatogenesis, tissue engineering, alginate, scaffold, 3D bioprinting

Supplementary material for this article is available online

Abstract

In vitro spermatogenesis (IVS) has already been successfully achieved in rodents by organotypic and soft matrix culture systems. However, the former does not allow single cell input, and the latter presents as a simple thick layer in which all cells are embedded. We explored a new culture system using a mouse model by employing an alginate-based hydrogel and 3D bioprinting, to control scaffold design and cell deposition. We produced testicular constructs consisting of printed cell-free scaffolds (CFS) with prepubertal testicular cells (TC) in their easy-to-access macropores. Here, the pores represented the only cell compartment (TC/CFS). Double-cell compartment testicular constructs were achieved by culturing magnetic-activated cell sorting-enriched epithelial cells in the pores of interstitial cell-laden scaffolds ($CD49f^{+}$/CLS). Cell spheres formed in the pores in the weeks following cell seeding on both CFS and CLS. Although restoration of the tubular architecture was not observed, patches of post-meiotic cells including elongated spermatids were found in 66% of TC/CFS. Differentiation up to the level of round spermatids and elongated spermatids was observed in all and 33% of $CD49f^{+}$/CLS constructs, respectively. Organ culture served as the reference method for IVS, with complete spermatogenesis identified in 80% of cultivated prepubertal tissue fragments. So far, this is the first report applying a 3D bioprinting approach for IVS. Further optimization of the scaffold design and seeding parameters might be permissive for tubular architecture recreation and thereby increase the efficiency of IVS in printed testicular constructs. While it remains to be tested whether the gametes generated on the alginate-based scaffolds can support embryogenesis following IVF, this IVS approach might be useful for (patho)physiological studies and drug-screening applications.

Introduction

Germ cells play a unique and fundamental role in human reproduction through their role in transmitting an individual's genetic information to the next generation. In males, spermatogenesis is the compartmentalized and tightly regulated process by which spermatozoa (haploid) are produced from spermatogonial stem cells (SSCs, diploid) involving mitosis, meiosis and spermiogenesis [1]. For nearly a century, researchers have been trying to replicate this process in culture and to achieve *in vitro* spermatogenesis (IVS) [2]. In 2011, a Japanese group headed by Professor Ogawa reconstituted mouse sperm production *in vitro* in an organ culture system. So far, this has been the most successful and widely used IVS method in animal models for immature and mature tissue. Simply by placing testicular tissue fragments at the gas–liquid interphase with culture medium consisting of α-minimum essential medium supplemented with Knockout serum replacement (KSR), sperm were obtained that fertilized oocytes following microinsemination, resulting in healthy fertile offspring [3]. However, the efficiency of that system was not

optimal. Finding robust culture conditions to ensure reliability and replicability was considered key. Reda *et al* emphasized the beneficial role of 10% KSR and recommended supplementation with melatonin and Glutamax for mouse IVS [4]. Despite the limited availability of fetal, newborn and prepubertal research material, advances were also made towards a human application in a study reporting proliferation of spermatogonia and maturation of the somatic compartment in cultured immature human testicular fragments [5]. Moreover, using the same methodology, maintenance of the somatic environment and proliferating germ cells have been observed in adult human testicular tissue [6, 7].

A key feature of this culture system is preservation of testicular cells (TCs) in their native 3D configuration: germ cells and Sertoli cells organized in seminiferous tubules and surrounded by interstitial cells. However, this is a limiting factor when manipulation of a particular cell type before culture is desired, for instance, to perform genetic modifications in a chosen cell population. IVS starting from dissociated TCs implies that an approach which restores the spatial arrangement of TCs in a 3D culture is needed.

Interestingly, Yokonishi *et al* demonstrated the capacity of neonatal mouse TCs to self-restore the testicular architecture *in vitro* after their dissociation into single cells without scaffold support [8]. The cells formed an aggregate in suspension culture and subsequently reorganized at the gas–liquid interphase into tubules containing Sertoli cells and germ cells. The germ cells were capable of differentiation, but did not progress beyond the meiotic phase [8]. The size of the aggregate and the lack of a microcirculatory system may have prevented further differentiation, because germ cells are vulnerable to hypoxic conditions and prone to apoptosis [9]. Others cultured suspensions of immature mouse TCs within a soft-agar culture system (SACS) or methylcellulose culture system (MCS), which resulted in the formation of several individual small-sized 3D cellular aggregates rather than a single big lump of cells [10, 11]. Embedding of the TCs in these soft matrices resulted in a beneficial effect to the cell–cell interactions, as after several weeks of culture, morphologically normal spermatozoa were obtained both in SACS and MCS. However, the aggregates lacked a tissue-specific organization. Since these culture systems present as a simple thick layer, they do not offer the possibility of creating more complex tissue-specific construct patterns. Moreover, SACS irreversibly encapsulates cells, ruling out easy recovery of living cells from the matrix for downstream applications.

Taken together, although useful culture systems have been established, a different approach is desired for the construction of customizable 3D tissue scaffolds enabling controlled cell disposition. A solution to this technical challenge might be near thanks to recent advances in tissue engineering that have enabled printing of biomimetic materials (so called 'bioink'), with cells and supportive components recreating complex 3D functional living tissues in a defined and organized manner, termed 'bioprinting'. The common strategies of bioprinting include inkjet or droplet printing, laser-assisted printing, stereolithography and extrusion-based printing [12–14]. Hydrogels, being high-water content polymeric networks, have played a pivotal role as printer bioink primarily in soft tissue engineering. Their similarity to native ECM, their easy handling and processing, and their tuneable biochemical and biophysical properties allows the biomimetic material to be tailored for the specific biomedical application, which critically impacts the cell fate imposed by the 3D cell microenvironment [15, 16]. Together with the extrusion parameters, they determine the construct rigidity and its cell encapsulation ability [17]. Alginate hydrogels are extensively used as a natural polymer for 3D bioprinting, but achieving shape fidelity is a known challenge while printing [18]. By combining the outstanding shear thinning properties of nanofibrillated cellulose with the fast crosslinking nature of alginate, a bioink was developed with remarkable printability [19]. The aim of this study was to explore a new IVS culture system using cell suspensions and self-designed alginate-based scaffolds printed by pneumatic microextrusion.

Materials and methods

Study design

The study involved the production of testicular constructs by culturing the total prepubertal TC population in easy-to-access macropores of printed cell-free scaffolds (CFS; single cell compartment) and magnetic-activated cell sorting (MACS)-enriched epithelial cells ($CD49f^{+}$) in pores of cell-laden scaffolds (CLS; double cell compartment) containing interstitial cells from juvenile mice. Donor material was obtained from the $C57BL/6J^{Acr3\text{-}EGFP}$ mouse differentiation reporter model to facilitate the monitoring of IVS [20]. Organ culture of prepubertal tissue served as reference method for IVS and was used to validate our evaluation methods.

Mice

Reporter transgenic male mice expressing EGFP in the acrosome ($C57BL/6J^{Acr3\text{-}EGFP}$) were generated in the Transgenic Unit of the Czech Center for Phenogenomics at the Institute of Molecular Genetics CAS [21]. Testes were obtained from prepubertal (<7 *dpp*) and adult (6 months old) male mice with approval of Animal Welfare Committee of the Czech Academy of Sciences (Animal Ethics Number 66866/2015-MZE-17214, 18 December 2015). A Material Transfer Agreement was obtained between the Institute of

Biotechnology, Czech Academy of Sciences and Vrije Universiteit Brussel on the 11th of November, 2017.

Donor testes from F1 hybrid (SV129 × C57BL/6J) juvenile (21 *dpp*) mice were obtained according to the guidelines of the Ethical Committee for the use of Laboratory Animals of the Vrije Universiteit Brussel (license LA2230395). Donor testes were decapsulated, cut in half and cryopreserved/thawed as described before [22].

Isolation, labeling and MACS of TCs

Testicular tissue from prepubertal C57BL/6J$^{Acr3\text{-}EGFP}$ mice was enzymatically digested using 1.0 mg ml^{-1} collagenase Ia (Sigma-Aldrich, Belgium), 0.5 mg ml^{-1} hyaluronidase (Sigma-Aldrich) and 0.5 mg ml^{-1} DNase (Sigma-Aldrich). The epithelial cells (SSCs and Sertoli cells) were enriched by MACS in accordance with the provider's instructions (Miltenyi Biotec, The Netherlands) using an antibody for CD49f (555735, FITC Rat anti-CD49f; BD Biosciences, Belgium) at a dilution of 40 μl per 10^6 cells in 100 μl. CD49f, also known as α-6-integrin, helps anchoring the epithelial cells to the laminin of the basement membrane [23, 24].

Testis fragments from juvenile mice were digested using only 1.0 mg ml^{-1} collagenase Ia, which resulted in tubular fragments and single interstitial cells. To enrich the latter, the fragments and single cells were separated by sedimentation at unit gravity.

The total number of viable cells was assessed after digestion and after MACS using trypan blue exclusion.

3D bioprinting of scaffolds

Sketchup software (Trimble, USA) was used to draw lattice structures (CFS: ⌀ 7 mm × 0.15 mm, strand distance 1.3 mm, strand thickness 0.6 mm; CLS: 3.5 mm × 3.5 mm × 0.15 mm, strand distance 1.1 mm, strand thickness 0.6 mm) and generate STereoLithography files. These files were translated into G-code using Heartware software (Cellink) and printed on glass microscope slides by a pneumatic-based microextrusion Inkredible + bioprinter (Cellink, Sweden) enclosed within a biosafety cabinet. To print CFS, Cellink-RGD bioink (nanocellulose-alginate hydrogel with an additional biofunctionalization of arginine-glycine-aspartate motives to improve cell attachment) was loaded into the cartridge and placed in the dispensing unit of the bioprinter. In order to print CLS, Cellink-RGD bioink was first diluted 1/10 with juvenile interstitial cells to obtain a final concentration of 10^7 cells ml^{-1}. Samples were homogenized by vortexing and air bubbles were removed by centrifugation. The bioink was dispensed using a 25-gauge conical nozzle (inner diameter = 0.437 mm nozzle; Subrex, USA) at room temperature with a pressure of 5–15 kPa and a plotting speed of 175–200 mm s^{-1}. After crosslinking with 100 mM aqueous $CaCl_2$ solution (Cellink) for 5 min, the scaffolds were rinsed with αMEM.

Culture of testicular tissue fragments and constructs

C57BL/6J$^{Acr3\text{-}EGFP}$ testicular tissue fragments, TC/CFS and CD49f$^+$/CLS were cultured up to 40 d, 48 d and 41 d, respectively, at 35 °C in a humidified atmosphere containing normal oxygen tension (21%) and 5% CO_2. The cell culture medium containing αMEM supplemented with 1× GlutaMAX (32571028, ThermoFisher, Belgium), 10% KSR (10828010, ThermoFisher), 10^{-7} M melatonin (M5250, Sigma-Aldrich) and 1% pen/strep (ThermoFisher) was replaced once a week [4].

The samples were cultured at the gas–liquid interface in 24-well plate hanging culture inserts (MCRP24H48, Merck, Belgium). While tissue pieces ($n = 3$ *Acr3-EGFP*$^-$ and $n = 2$ *Acr3-EGFP*$^+$) were placed directly on the membrane, CFS were transferred on a 0.35% agarose support which prevented cell attachment to the membrane. CLS were slid into a 0.35% agarose socket. The socket was created by pipetting 25 μl of liquid agarose around a printed mold (dimensions 42 mm × 42 mm × 1.5 mm) placed on an agarose support to fit the scaffold and ensure proper cell seeding in the macropores. The testicular constructs were prepared by seeding unsorted TCs on CFS ($n = 3$ *Acr3-EGFP*$^-$ and $n = 3$ *Acr3-EGFP*$^+$) or CD49f$^+$ cells on and CLS ($n = 3$ *Acr3-EGFP*$^+$) at a density of 2 × 10^4 cells mm^{-2} scaffold. The non-invasive evaluation of differentiation in testicular tissue fragments and general culture follow-up were performed using an inverted fluorescence microscope (Olympus, Belgium) and ToupView (ToupTek Photonics, China) software.

Immunofluorescence and histochemistry

To evaluate the efficiency of epithelial cell enrichment, the percentages of Sertoli cells and spermatogonia were determined on 4% paraformaldehyde-fixed cytospins of both the CD49f$^+$ and CD49f$^-$ fractions using the specific markers SOX9 and MVH, respectively [25]. Antigen retrieval was performed using a 0.01 M citrate buffer (pH 6.0) containing 0.05% Tween-20 (Sigma-Aldrich) in a water bath at 95 °C during 30 min. The samples were blocked with blocking solution containing 10% normal donkey serum (NDS; Bioconnect, The Netherlands) in PBS for 30 min. Rabbit polyclonal anti-MVH primary antibody (ab13840, 2.5 μg ml^{-1}; Abcam, UK) or rabbit polyclonal anti-SOX9 primary antibody (AB5535, 5 μg ml^{-1}; Merck) was added and incubated overnight at 4 °C. The primary antibodies were diluted in blocking solution containing 10% NDS and 5% BSA (w/v) in PBS. The next day, the cytospins were incubated with donkey anti-rabbit 488 secondary antibody (A21206, Life technologies, 1:200) diluted in PBS for 1 h at RT. All washing steps were performed in

PBS. The cytospins were mounted with DAPI (4′, 6-Diamidino-2-Phenylindole; S36937, Invitrogen) and the coverslips were sealed with nail polish. The experiment was performed in triplicate. For each replicate, the amount of positive and negative cells was counted using ImageJ software (National Institute of Health, USA) on three representative fields taken with an inverted fluorescence microscope (Olympus) and Cell^F software (Olympus).

At the end of the culture period, the testicular tissue fragments and testicular constructs were fixed in acidified alcoholic formalin (VWR, Belgium), embedded in paraffin and cut into 5 μm thick sections at different depths. Sections were stained with periodic acid-Schiff (PAS; VWR) in accordance with the manufacturer's protocol and haematoxylin in order to perform morphological evaluation of the cultured samples. Different types of germ cells were identified based on morphological characteristics previously described [26].

To confirm the presence of post-meiotic germ cells, co-staining for EGFP and CREM or PNA was performed. Antigen retrieval using a 0.01 M citrate buffer (pH 6.0) containing 0.05% Tween-20 was performed in a water bath at 95 °C for 30 min. The endogenous peroxidase enzyme was blocked by methanol/3% H_2O_2 for 30 min at RT. The sections were blocked with blocking solution containing normal chicken serum 20% (v/v) (NChS, Sigma) and 5% BSA (w/v) in TBS. Goat polyclonal anti-GFP primary antibody (ab13840, 5 μg ml^{-1}; Abcam) and rabbit polyclonal anti-CREM primary antibody (SC-440, 1 μg ml^{-1}; Bio-Connect, The Netherlands) were added. The primary antibodies were diluted in the blocking solution (TBS/NChS/BSA) and the sections were incubated overnight at 4 °C. For CREM immunostaining, the sections were incubated with horseradish peroxidase (HRP)-conjugated chicken anti-rabbit secondary antibody (SC-2963, 5 μg ml^{-1}; Bio-Connect) diluted in blocking solution (TBS/NChS/BSA) for 30 min at RT. The TSA™ Cy3 Plus System (NEL741001KT, Perkin Elmer Life Sciences, Boston, USA) was applied according to the manufacturer's instructions for 3 min. For EGFP immunostaining, the sections were incubated with donkey anti-goat 488 secondary antibody (A11055, Life technologies, 1:200, final concentration 1 μg ml^{-1}) diluted in TBS for 60 min at RT. All washing steps were performed in TBS. When the acrosome needed to be visualized, the sections were incubated with Alexa Fluor 594-conjugated peanut agglutinin (PNA; 5 μg ml^{-1}; ThermoFisher) diluted in TBS for 1h30 at RT. The sections were mounted with DAPI and the coverslips were sealed with nail polish.

Adult and prepubertal mouse testicular tissue sections were used as control. As background control, normal rabbit immunoglobulin G (IgG, sc-2027, Bio-Connect), normal goat IgG (sc-2028, Bio-Connect) or normal mouse IgG (sc-2025, Bio-Connect) were applied instead of the primary antibody.

Statistical analysis

Multiple t-test (Holm-Sidak method to correct for multiple comparison) was used to statistically analyze the enrichment of the epithelial fraction by MACS. Data are presented as mean values ± standard deviation. A difference was considered to be statistically significant if the p-value was $\leqslant 0.05$.

Results

Organ culture as reference method for IVS

Non-invasive monitoring of germ cell differentiation

In adult C57BL/6J$^{Acr3\text{-}EGFP}$ testis, EGFP is located in the cytoplasm of meiotic cells and in the (forming) acrosome of post-meiotic cells, thus Acr3-EGFP expression can be used as a reporter of germ cell differentiation, supplemental figure 1(A) is available online at stacks.iop.org/BF/11/035011/mmedia. In order to study the timing and extent of Acr3-EGFP expression in cultured prepubertal Acr3-EGFP testes, testicular fragments ($n = 5$) were regularly evaluated throughout a 40 d period. Both *Acr3-EGFP*$^{-}$ ($n = 2$) and *Acr3-EGFP*$^{+}$ ($n = 3$) testicular tissues did not show positive EGFP fluorescent signal on day 0, supplemental figure 1(A). From the second week onwards, the formation of a lumen could be seen in both *Acr3-EGFP*$^{-}$ and *Acr3-EGFP*$^{+}$ testicular tissues indicating tubular growth. On day 12, EGFP fluorescence was observed inside some tubules of *Acr3-EGFP*$^{+}$ fragments, in contrast to *Acr3-EGFP*$^{-}$ fragments which exhibited no fluorescence. Throughout the rest of the culture period, the number of tubules with Acr3-EGFP labeling increased in *Acr3-EGFP*$^{+}$ testicular fragments, whereas, on day 40, EGFP expression was, as expected, not detected in *Acr3-EGFP*$^{-}$ testicular tissues, figure 1(A).

In-depth examination of germ cell differentiation

PAS/hematoxylin staining of adult *Acr3-EGFP*$^{+}$ tissue showed that round spermatids had a nucleus with a characteristic dot, and were partially covered by an acrosomal cap while elongated spermatids have a flattened nucleus with an acrosome over the anterior region, supplemental figure 1(B). Before organ culture, SSCs were most advanced cell type in the prepubertal C57BL/6J$^{Acr3\text{-}EGFP}$ testicular fragments, supplemental figure 1(B). Histology of cultured prepubertal C57BL/6J$^{Acr3\text{-}EGFP}$ confirmed tubular growth with lumen formation and the presence of post-meiotic cells in two out of three *Acr3-EGFP*$^{-}$ and two out of two *Acr3-EGFP*$^{+}$ testicular tissues after 40 d of culture, figure 1(B). One *Acr3-EGFP*$^{-}$ replicate was sclerotic.

Because cell identification by histology strongly relies on tissue architecture, we performed a double immunostaining for CREM (round spermatid marker) and EGFP to differentiate between round and elongated spermatids. CREM staining in adult

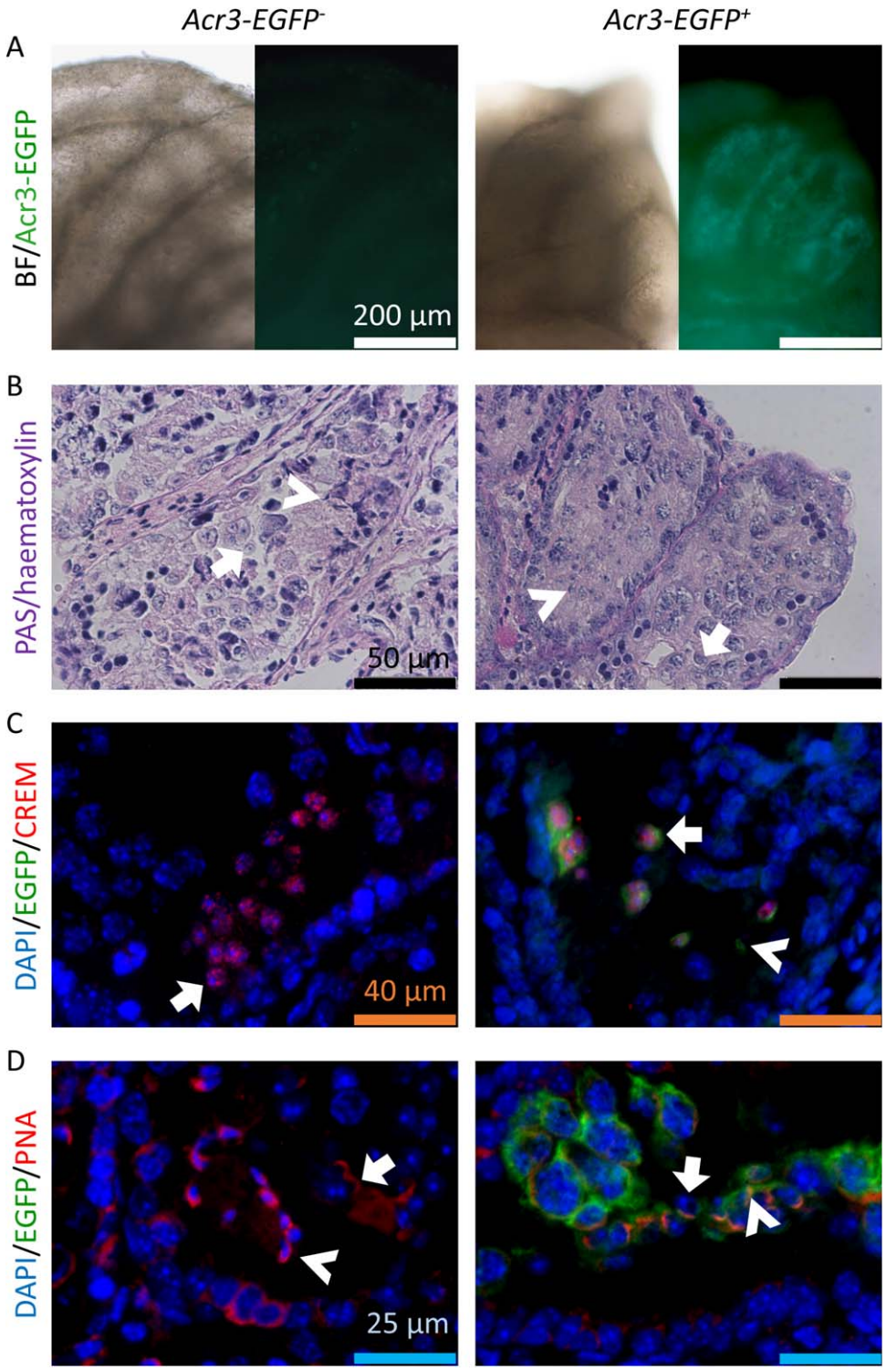

Figure 1. Organ culture as a reference method for IVS**.** Tubular maturation and formation of post-meiotic germ cells were observed in prepubertal *Acr3-EGFP*$^{-}$ (left column) and *Acr3-EGFP*$^{+}$ (right column) testicular tissues after 40 d in culture. (A) Brightfield (BF) showing tubules with Acr3-EGFP expression in *Acr3-EGFP*$^{+}$ cells, but not in *Acr3-EGFP*$^{-}$ cells. (B) PAS with hematoxylin counterstaining showing the histology of cultured tissues. (C) Co-immunostaining of EGFP (green) and CREM (red) was used to specifically identify round spermatids. (D) Co-staining with an antibody against EGFP (green) and the PNA (red) dye highlighted the acrosomal cap in round spermatids and the acrosome of elongated spermatids. Cell nuclei were stained with DAPI (blue). Round and elongated spermatids are indicated by an arrow and arrow head, respectively.

Acr3-EGFP^{+} tissue was localized to the nuclei of round spermatids while the elongated spermatids were CREM^{-}, supplemental figure 1(C). EGFP specifically stains the cytoplasm (predominantly the acrosomal cap and acrosome) of round and elongated spermatids which corresponds with the PNA staining, supplemental figure 1(D). *In vitro* generated round and elongated spermatids could selectively and reliably be identified based on the shape of the nucleus, the status of the acrosome visualized by PNA and the presence of

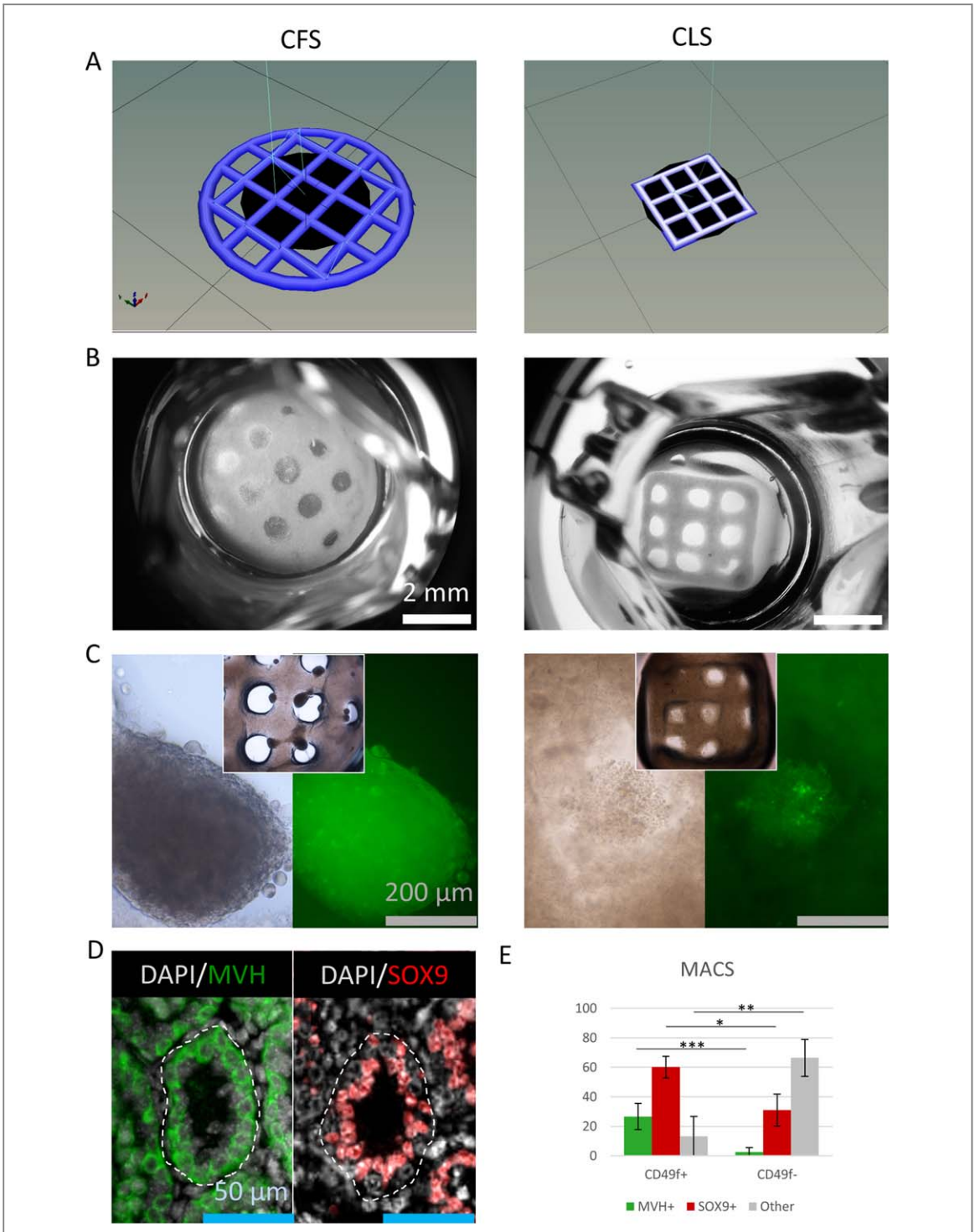

Figure 2. Fabrication of testicular constructs using bioprinted scaffolds. (A) and (B) The 3D design (A) and printout (B) of CFS (cell-free scaffolds; left column) and CLS (cell-laden scaffolds; right column). (C) Gross morphology (left panels) and Acr3-EGFP expression (right panels) of the spheroids growing on the CFS and CLS at culture day 48 and day 41, respectively. The inserts depict low-magnification overviews. (D) The seminiferous epithelium of prepubertal mice consists of spermatogonia, including spermatogonial stem cells, and Sertoli cells expressing MVH^+ (green) and $SOX9^+$ (red), respectively. Cell nuclei were stained with DAPI (white). (E) MVH^+ and $SOX9^+$ cells made up the vast majority of the MACS-selected $CD49f^+$ fraction which was seeded on CLS. The $CD49f^-$ fraction consisted mainly of other cells, likely interstitial cells. $^*p = 0.02$, $^{**}p = 0.01$ and $^{***}p = 0.007$.

the CREM marker in all healthy *Acr3-EGFP*$^+$ and *Acr3-EGFP*$^-$ tissues, figures 1(C), (D).

Fabrication of testicular constructs using bioprinted scaffolds

CFS were printed in the shape of a circle with an internal lattice structure that formed pores, figures 2(A), (B). Unsorted TCs were seeded, which over the following days clustered together and formed spheroids within the CFS pores. Occasionally, spheroids from different pores formed connections with each other, figure 2(C). After 48 d in culture, Acr3-EGFP expression was observed in cells of *Acr3-EGFP*$^+$

TC/CFS constructs, figure 2(C). Acr3-EGFP expression was absent in *Acr3-EGFP*$^{-}$ TC/CFS.

CLS were printed with smaller dimensions compared to CFS to minimize the empty space between the interstitial cells in the scaffold and the CD49f^{+} cells which were seeded in the macropores, figures 2(A), (B). CD49f^{+} cells also formed spheroids during culture and contained EGFP^{+} cells indicating germ cell differentiation, figure 2(C).

When studying the seminiferous epithelium of prepubertal animals, only spermatogonia, including SSCs, and Sertoli cells can be seen, figure 2(D). Characterization of the MACS-selected populations showed more epithelial cells were found in the CD49f^{+} fraction than in the CD49f^{-} fractions (86.8 ± 13.4 versus 33.6 ± 12.5; $p = 0.007$). Specifically, the CD49f^{+} fraction contained higher portions of SOX9^{+} Sertoli cells (60.1 ± 7.2 and 26.6 ± 8.8; $p = 0.02$) and MVH^{+} spermatogonia (31.0 ± 10.8 and 2.6 ± 3.1; $p = 0.01$), compared with CD49f^{-} fractions, figure 2(E).

Spermatogenesis in bioprinted testicular constructs

Immunofluorescent and immunohistochemical staining confirmed the presence of post-meiotic germ cells in four out of six TC/CFS (66%) and three out of three CD49f^{+}/CLS (100%) testicular constructs. Round spermatids showing cytoplasmic EGFP expression and nuclear CREM expression were observed in all *Acr3-EGFP*$^{+}$ TC/CFS and CD49f^{+}/CLS testicular constructs, figure 3(A). Only one out of three *Acr3-EGFP*$^{-}$ TC/CFS testicular constructs contained round spermatids.

In addition, co-staining for EGFP and PNA differentiated the presence of round and elongated spermatids in 66% of TC/CFS and 33% of CD49f^{+}/CLS testicular constructs. Specifically, while all *Acr3-GFP*$^{+}$ TC/CFS contained elongated spermatids with an acrosome containing EGFP and/or binding of PNA, only one *Acr3-EGFP*$^{-}$ TC/CFS and one CD49f^{+}/CLS construct contained such advanced germ cells, figure 3(B). EGFP was not detected in *Acr3-EGFP*$^{-}$ TC/CFS.

Sections of TC/CFS and CD49f^{+}/CLS stained with PAS/hematoxylin support the immunostaining and histochemistry findings on germ cell differentiation, figure 3(C). However studies of the overall morphology of TC/CFS and CD49f^{+}/CLS spheroids revealed that they did not display a seminiferous tubule-like histology, but either contained patches of differentiating germ cells or, more often, had a fibrotic appearance, figure 3(D). The CLS still contained interstitial cells after 41 d of culture, but their density in the hydrogel decreased over time, figure 3(E).

Discussion

Tissue engineering has grown in the last few decades as a new interdisciplinary scientific field combining principles of material chemistry, engineering, medicine and life sciences. 3D bioprinting is a rapidly emerging technology in tissue engineering and has already been used for generation and transplantation of several tissues, such as multi-layered skin and cartilaginous structures [27]. Recently, a pioneering reproductive study employed 3D bioprinting to design scaffolds which supported mouse follicle growth. Moreover, these bioprosthetic ovaries gave rise to *in vivo* functional ovarian implants in surgically sterilized mice [28]. We subsequently asked whether this technique could be applied to male reproductive biology research. For rodent IVS, there are already functional systems of which the organ culture method is the most reliable. However, the field would welcome a new IVS system that would allow the creation of customized 3D tissue constructs with controlled scaffolds design and cell deposition.

To address this demand, we first generated organ cultures of C57BL/6J$^{\text{Acr3-EGFP}}$ testicular tissue fragments as an IVS reference system with culture conditions according to Reda *et al* [4]. This approach gave us the opportunity to reliably validate our germ cell differentiation assays. We reported spermatogenesis up to the level of elongated spermatids by detecting Acr3-EGFP expression combined with specific identification of post-meiotic germ cells in 80% of testicular tissue fragments. Despite slow-freezing and thawing the fragments prior to culture, results comparable to the study of Reda *et al* were obtained, which reported spermatogenesis in 67% of the freshly cultured tissue fragments. This is also in accordance with an earlier study which demonstrated that cryopreservation of testis tissues followed by organ culture maintains the efficiency of IVS [29]. Next, we focussed on developing testicular constructs using 3D bioprinting and C57BL/6J$^{\text{Acr3-EGFP}}$ testicular single-cell suspensions.

Yokonishi *et al* previously demonstrated that mouse TCs cultured at the gas–liquid interphase have the ability to reconstruct the testicular architecture in aggregates [8]. We combined this *in vitro* reconstruction technique with alginate-based CFS and obtained single cell-compartment testicular constructs (TC/CFS) with small-sized spheroids attached to the lining of the macropores. It is remarkable that we observed post-meiotic germ cells including elongated spermatids in the TC/CFS, considering meiotic cells were the most advanced cell type observed by Yokonishi *et al* in their reconstructed tissues. This difference could be explained by the different dimensions of the samples and/or medium supplements used in both studies. Cells growing in flatter structures are less likely to experience hypoxia. Recently, it was shown that spreading tissue two-dimensionally into a disc-shape with singly-layered seminiferous tubules could

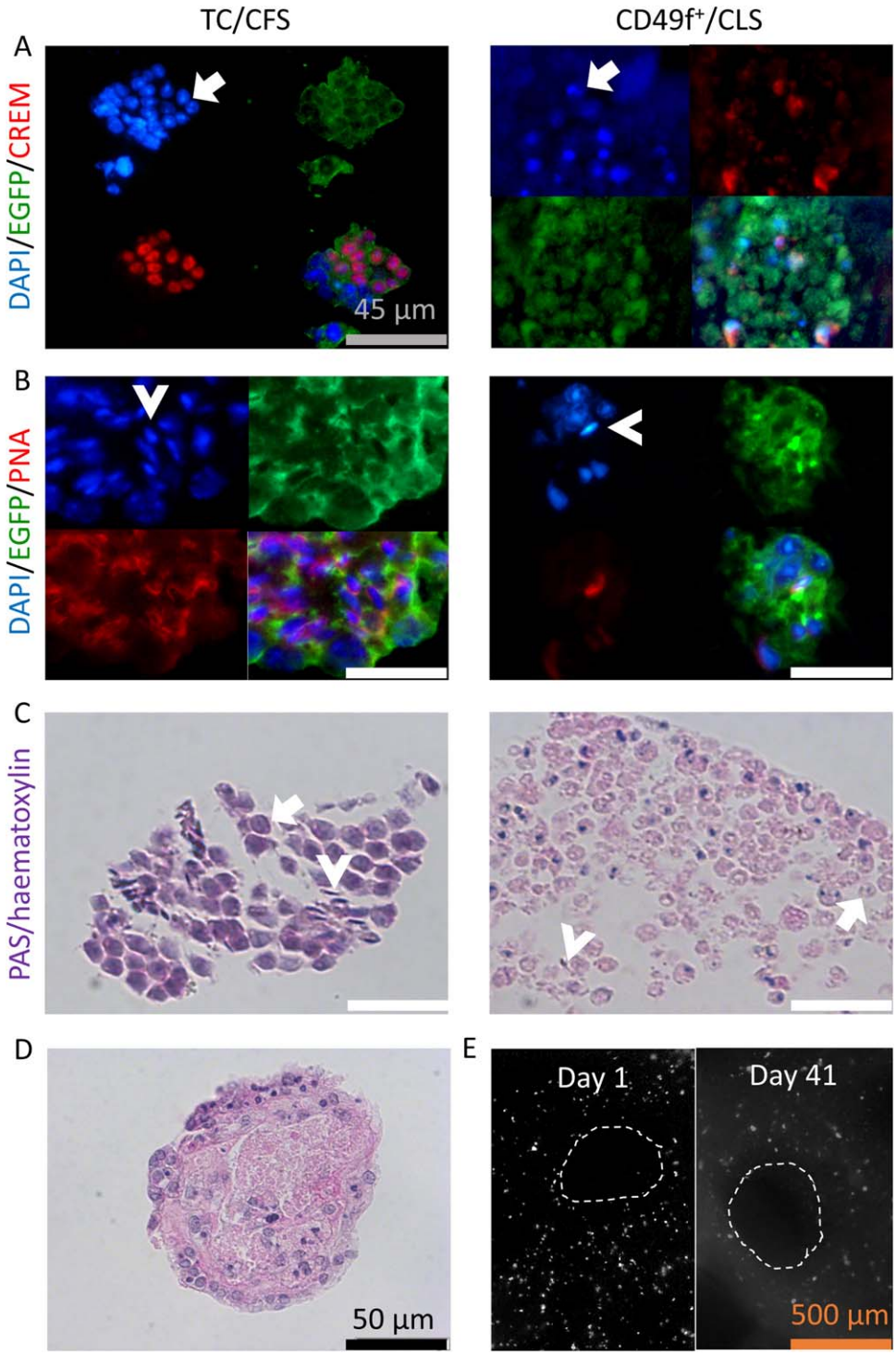

Figure 3. Spermatogenesis in bioprinted testicular constructs. Histochemical and immunofluorescent staining of TC/CFS (testicular cell/cell-free scaffolds; left column) and CD49f$^+$/CLS (cell-laden scaffolds; right column) at culture days 48 and day 41, respectively. (A) and (B) The detection of EGFP$^+$ (green)/CREM$^+$ (red) (A) and EGFP$^+$ (green)/PNA$^+$ (red) cells (B) in TC/CFS and CD49f$^+$/CLS testicular constructs confirmed the formation of round (arrow) and elongated (arrow heads) spermatids. Counter-staining was performed with DAPI (blue). (C) Germ cells occurred in patches in the spheroids as seen after PAS/hematoxylin staining of TC/CFS and CD49f$^+$/CLS. (D) Spheroids without germ cells had a fibrotic appearance. (E) CLS still contained interstitial cells at the end of the culture period, though at a lower density compared to the first day of culture. Dotted lines delineate pores of CLS. Cell nuclei were stained with DAPI (white).

prevent central necrosis in organ culture [30]. Yokonishi's reconstructed tissues had a diameter of roughly 2 mm, compared with our spheroids which measured approximately 300 μm. In addition, instead of adding GNDF, the culture medium was supplemented with GlutaMAX and melatonin, which have an anti-cytotoxic effect and positively influence germ cell differentiation in the organ culture system [4]. Both differences may have had a beneficial effect on the differentiation of SSCs towards post-meiotic germ cells.

Nevertheless, it is important to note that we did not observe tubular structures. This could be due to sub-optimal cell densities, whereby cell–cell and paracrine inhibiting/activating interactions which are crucial for tubular reorganization *in vitro* are deficient, as was observed in an earlier study using rat TCs [31]. This could also explain why post-meiotic germ cells were found only in a few spheroids per TC/CFS replicate. Higher cell densities might favor the formation of better-connected spheroids with recognizable testicular architecture resulting in more efficient IVS.

While the scaffold in TC/CFS merely serves as structural support and restoration of the tubular structures is reliant on the self-organizational abilities of the TCs, whereas culturing tubular cells in the macropores of interstitial CLS directly recreates the two main testicular compartments. This would be of interest for adult human and other testicular organoid models particularly because mature somatic cells appear unable to initiate reorganization of testicular structures [31, 32]. Our reasons for selecting to encapsulate juvenile interstitial cells were twofold: (i) juvenile donors yield higher cell numbers per testis compared to prepubertal donors, which is especially important for 3D bioprinting [33], and (ii) since juvenile interstitial cells are more mature and already supporting active spermatogenesis, it was assumed that secreted factors would better stimulate tubular cells in the scaffold macropores. This idea is reinforced by previously published data showing that donor-derived immature tubular cells were able to restart spermatogenesis in empty seminiferous tubules of adult recipient mice with an intact testicular interstitium [34].

The efficiency of IVS (up to the formation of elongated spermatids) in publications using organ culture (67%) and soft agarose culture (68%) is comparable to our TC/CFS (66%), but higher compared to CD49f$^+$/CLS constructs (33%) [4, 11]. It should be kept in mind, however, that this study has some shortcomings. Firstly, it is based on a low sample size due to the laborious procedure needed to produce the transgenic mice. Secondly, there is a considerable decrease in density of interstitial cells in CLS over time and this may be due to hydrogel incompatibility. Because alginate hydrogels are inert to cells, we opted to use alginate with RGD motifs which mimics the binding site within fibronectin and several other extracellular matrix proteins to improve cellular adaptability [18]. However, interstitial cells might prefer to be encapsulated in hydrogels that better represent the complexity of natural extracellular matrix [35]. Such printable hydrogels could be tested to improve the outcome of CD49f$^+$/CLS cultures. It has been shown that the presence of all somatic TC types is required to achieve IVS [10]. Even though interstitial cell loss occurred, post-meiotic germ cells were detected in all CD49f$^+$/CLS replicates. It is possible that the contaminating non-epithelial cells in the CD49f$^+$ fraction were responsible or at least contributed to the support of the germ cell differentiation noted in CD49f$^+$/CLS. Fluorescence-activated cell sorting could be used instead of MACS to improve the efficiency of cell separation [36]. Moreover, as the epithelial SOX9$^+$ cells were not restricted to the CD49f$^+$ fraction, an additional Sertoli cell-specific marker such as FSHR could be considered in future experiments [37]. Optimization of CD49f$^+$/CLS cultures might also be achieved by striving for CLS with more anatomically correct dimensions to maintain a balanced composition of each cell type. For instance, the pores were intentionally smaller in CLS (300–500 μm) than CFS (500–700 μm), but still bigger than adult mouse seminiferous tubules (~200 μm). In the 3D printed bioprosthetic ovary study, they demonstrated that scaffold pore architecture is a crucial variable for optimal ovarian murine follicle growth and differentiation *in vitro*. The results from this study led to the conclusion that follicle spreading was limited and the survival of the follicles increased when the scaffold-follicle interaction increased by manipulating the pore geometry [28]. Finally, the current study did not focus on assessing the competency of *in vitro* produced gametes nor their fidelity. Alterations at the (epi-)genetic level can have serious consequences for early development or long-term health of the resultant offspring [38]. Thus, assessments of the fertility and chromosomal and epigenetic normality are warranted, especially if the intended use is of a clinical nature [39]. Interestingly, it was previously shown that *in vitro* generated sperm from frozen-thawed mouse testicular tissues used for microinsemination resulted in healthy and fertile offspring [29].

Conclusion

This study is the first to report IVS in testicular constructs created by seeding single cell suspensions on 3D bioprinted CFS and CLS. In addition to being used as a fertility management technique for cancer survivors, it could promote advances in (patho) physiological studies by reuniting TCs after gain- or loss-of-function experiments. Testicular constructs could also have an industrial application. Inspired by bioprinting-based hydrogel microarrays for cells and cellular spheroids [40, 41], high-throughput fabrication of testicular constructs on chips could facilitate screening for fertility therapeutics and disruptors [42, 43]. A major advantage of the use of freeform printed scaffolds is the opportunity to customize the size and shape of the *in vitro* created tissues and decide the location and composition of its cell compartments. These features are especially interesting for the field of whole-organ (re)engineering. Lab-grown testes could restore natural reproductive functions in infertile patients, for instance anorchic patients or patients with a genitourinary trauma involving the testes,

frequently caused by sports activities, road accidents or work injuries [44–46].

Acknowledgments

We are grateful to S Gündogan, P Hilven and F Van Haelst from the Vrije Universiteit Brussel for their technical assistance and to K Loveland and P Whiley from Monash University for English language editing. Also, we express our gratitude to M Okabe for the kind gift of Acr3-EGFP plasmid and to D Prukova and I Beck from the Institute of Molecular Genetics for their assistance in the generation of transgenic mouse reporters. This work was supported by research grants from the Scientific Research Foundation Flanders (FWO), University Hospital Brussels (scientific fund Willy Gepts), the Vrije Universiteit Brussel (Methusalem grant), Grant Agency of the Czech Republic (GA-18-11275S), project 'BIOCEV' (CZ.1.05/1.1.00/02.0109) and the Institute of Biotechnology (RVO: 86652036). Y Baert is a postdoctoral fellow of the FWO.

ORCID iDs

Yoni Baert https://orcid.org/0000-0002-9169-548X

References

[1] Shalet S M 2009 Normal testicular function and spermatogenesis *Pediatr. Blood Cancer* **53** 285–8
[2] Martinovitch P N 1937 Development *in vitro* of the mammalian gonad *Nature* **139** 413
[3] Sato T, Katagiri K, Gohbara A, Inoue K, Ogonuki N, Ogura A, Kubota Y and Ogawa T 2011 *In vitro* production of functional sperm in cultured neonatal mouse testes *Nature* **471** 504–7
[4] Reda A, Albalushi H, Montalvo S C, Nurmio M, Sahin Z, Hou M, Geijsen N, Toppari J, Söder O and Stukenborg J-B 2017 Knock-out serum replacement and melatonin effects on germ cell differentiation in murine testicular explant cultures *Ann. Biomed. Eng.* **45** 1783–94
[5] de Michele F, Poels J, Weerens L, Petit C, Evrard Z, Ambroise J, Gruson D and Wyns C 2016 Preserved seminiferous tubule integrity with spermatogonial survival and induction of sertoli and leydig cell maturation after long-term organotypic culture of prepubertal human testicular tissue *Hum. Reprod.* **32** 1–14
[6] Roulet V, Denis H, Staub C, Le Tortorec A, Delaleu B, Satie A P, Patard J J, Jégou B and Dejucq-Rainsford N 2006 Human testis in organotypic culture: application for basic or clinical research *Hum. Reprod.* **21** 1564–75
[7] Jørgensen A, Young J, Nielsen J E, Joensen U N, Toft B G, Rajpert-De Meyts E and Loveland K L 2014 Hanging drop cultures of human testis and testis cancer samples: a model used to investigate activin treatment effects in a preserved niche *Br. J. Cancer* **110** 2604–14
[8] Yokonishi T, Sato T, Katagiri K, Komeya M, Kubota Y and Ogawa T 2013 *In vitro* reconstruction of mouse seminiferous tubules supporting germ cell differentiation *Biol. Reprod.* **89** 1–6
[9] Farias J G, Bustos-Obregon E, Orellana R, Bucarey J L, Quiroz E and Reyes J G 2005 Effects of chronic hypobaric hypoxia on testis histology and round spermatid oxidative metabolism *Andrologia* **37** 47–52
[10] Stukenborg J-B, Schlatt S, Simoni M, Yeung C-H, Elhija M A, Luetjens C M, Huleihel M and Wistuba J 2009 New horizons for *in vitro* spermatogenesis? An update on novel three-dimensional culture systems as tools for meiotic and post-meiotic differentiation of testicular germ cells *Mol. Hum. Reprod.* **15** 521–9
[11] Abu Elhija M, Lunenfeld E, Schlatt S and Huleihel M 2012 Differentiation of murine male germ cells to spermatozoa in a soft agar culture system *Asian J. Androl.* **14** 285–93
[12] Murphy S V and Atala A 2014 3D bioprinting of tissues and organs *Nat. Biotechnol.* **32** 773–85
[13] Marx V 2015 Organs from the lab *Nature* **522** 373
[14] Pati F, Ha D-H, Jang J, Han H H, Rhie J-W and Cho D-W 2015 Biomimetic 3D tissue printing for soft tissue regeneration *Biomaterials* **62** 164–75
[15] Ma Y, Lin M, Huang G, Li Y, Wang S, Bai G, Lu T J and Xu F 2018 3D spatiotemporal mechanical microenvironment: a hydrogel-based platform for guiding stem cell fate *Adv. Mater.* **30** 1705911
[16] Huang G, Li F, Zhao X, Ma Y, Li Y, Lin M, Jin G, Lu T J, Genin G M and Xu F 2017 Functional and biomimetic materials for engineering of the three-dimensional cell microenvironment *Chem. Rev.* **117** 12764–850
[17] Billiet T, Vandenhaute M, Schelfhout J, Van Vlierberghe S and Dubruel P 2012 A review of trends and limitations in hydrogel-rapid prototyping for tissue engineering *Biomaterials* **33** 6020–41
[18] Andersen T, Auk-Emblem P and Dornish M 2015 3D cell culture in alginate hydrogels *Microarrays* **4** 133–61
[19] Markstedt K, Mantas A, Tournier I, Martínez Ávila H, Hägg D and Gatenholm P 2015 3D bioprinting human chondrocytes with nanocellulose alginate bioink for cartilage tissue engineering applications *Biomacromolecules* **16** 1489–96
[20] Nakanishi T, Ikawa M, Yamada S, Parvinen M, Baba T, Nishimune Y and Okabe M 1999 Real-time observation of acrosomal dispersal from mouse sperm using GFP as a marker protein *FEBS Lett.* **449** 277–83
[21] Jankovicova J *et al* 2016 Characterization of tetraspanin protein CD81 in mouse spermatozoa and bovine gametes *Reproduction* **152** 785–93
[22] Baert Y, Goossens E, Van Saen D, Ning L, in't Veld P and Tournaye H 2012 Orthotopic grafting of cryopreserved prepubertal testicular tissue: in search of a simple yet effective cryopreservation protocol *Fertil. Steril.* **97** 1152–7.e2
[23] Salanova M, Ricci G, Boitani C, Stefanini M, De Grossi S and Palombi F 1998 Functional contacts between sertoli cells in normal and aspermatogenic rat seminiferous epithelium contain $\alpha 6\beta 1$ integrins, and their formation is controlled by follicle-stimulating hormone1 *Biol. Reprod.* **58** 371–8
[24] Shinohara T, Avarbock M R and Brinster R L 1999 1- and 6-integrin are surface markers on mouse spermatogonial stem cells *Proc. Natl Acad. Sci.* **96** 5504–9
[25] Alves-Lopes J P, Söder O and Stukenborg J B 2018 Use of a three-layer gradient system of cells for rat testicular organoid generation *Nat. Protocols* **13** 248–59
[26] Ahmed E A and de Rooij D G 2009 *Staging of Mouse Seminiferous Tubule Cross-Sections* ed S Keeney vol 558 (Totowa, NJ: Humana Press)
[27] Aljohani W, Ullah M W, Zhang X and Yang G 2018 Bioprinting and its applications in tissue engineering and regenerative medicine *Int. J. Biol. Macromol.* **107** 261–75
[28] Laronda M M, Rutz A L, Xiao S, Whelan K A, Duncan F E, Roth E W, Woodruff T K and Shah R N 2017 A bioprosthetic ovary created using 3D printed microporous scaffolds restores ovarian function in sterilized mice *Nat. Commun.* **8** 15261
[29] Yokonishi T *et al* 2014 Offspring production with sperm grown *in vitro* from cryopreserved testis tissues *Nat. Commun.* **5** 4320
[30] Kojima K *et al* 2018 Neonatal testis growth recreated *in vitro* by two-dimensional organ spreading *Biotechnol. Bioeng.* **115** 3030–41

[31] Alves-Lopes J P, Söder O and Stukenborg J-B 2017 Testicular organoid generation by a novel *in vitro* three-layer gradient system *Biomaterials* **130** 76–89
[32] Baert Y, De Kock J, Alves-Lopes J P, Söder O, Stukenborg J-B and Goossens E 2017 Primary human testicular cells self-organize into organoids with testicular properties *Stem Cell Rep.* **8** 30–8
[33] Reid J A, Mollica P A, Johnson G D, Ogle R C, Bruno R D and Sachs P C 2016 Accessible bioprinting: adaptation of a low-cost 3D-printer for precise cell placement and stem cell differentiation *Biofabrication* **8** 025017
[34] Shinohara T, Orwig K E, Avarbock M R and Brinster R L 2003 Restoration of spermatogenesis in infertile Mice by sertoli cell Transplantation1 *Biol. Reprod.* **68** 1064–71
[35] Pati F, Jang J, Ha D-H, Won Kim S, Rhie J-W, Shim J-H, Kim D-H and Cho D-W 2014 Printing three-dimensional tissue analogues with decellularized extracellular matrix bioink *Nat. Commun.* **5** 3935
[36] Geens M, Van de Velde H, De Block G, Goossens E, Van Steirteghem A and Tournaye H 2007 The efficiency of magnetic-activated cell sorting and fluorescence-activated cell sorting in the decontamination of testicular cell suspensions in cancer patients *Hum. Reprod.* **22** 733–42
[37] O'Shaughnessy P J, Monteiro A, Verhoeven G, De Gendt K and Abel M H 2010 Effect of FSH on testicular morphology and spermatogenesis in gonadotrophin-deficient hypogonadal mice lacking androgen receptors *Reproduction* **139** 177–84
[38] el Hajj N and Haaf T 2013 Epigenetic disturbances in *in vitro* cultured gametes and embryos: implications for human assisted reproduction *Fertil. Steril.* **99** 632–41
[39] Hendriks S, Dondorp W, de Wert G, Hamer G, Repping S and Dancet E A F 2015 Potential consequences of clinical application of artificial gametes: a systematic review of stakeholder views *Hum. Reprod. Update* **21** 297–309
[40] Ma Y, Ji Y, Huang G, Ling K, Zhang X and Xu F 2015 Bioprinting 3D cell-laden hydrogel microarray for screening human periodontal ligament stem cell response to extracellular matrix *Biofabrication* **7** 044105
[41] Ling K, Huang G, Liu J, Zhang X, Ma Y, Lu T J and Xu F 2015 Bioprinting-based high-throughput fabrication of three-dimensional MCF-7 human breast cancer cellular spheroids *Engineering* **1** 269–74
[42] Del Vento F, Vermeulen M, de Michele F, Giudice M G, Poels J, des Rieux A and Wyns C 2018 Tissue engineering to improve immature testicular tissue and cell transplantation outcomes: one step closer to fertility restoration for prepubertal boys exposed to gonadotoxic treatments *Int. J. Mol. Sci.* **19** E286
[43] Parks Saldutti L 2013 *In vitro* testicular toxicity models: opportunities for advancement via biomedical engineering techniques *ALTEX* **30** 353–77
[44] Hudolin T and Hudolin I 2003 Surgical management of urogenital injuries at a war hospital in Bosnia–Hrzegovina, 1992–1995 *J. Urol.* **169** 1357–9
[45] Pavan N, d'Aloia G, Bucci S, de Concilio B, Mazzon G, Ollandini G, Trombetta C and Liguori G 2014 Fertility preservation after bilateral severe testicular trauma *Asian J. Androl.* **16** 650
[46] Silber S J 1978 Transplantation of a human testis for anorchia *Fertil. Steril.* **30** 181–7